The Target System Baseline

H.G. Kirk (*BNL*) and K.T. McDonald (*Princeton U.)*
(Feb. 4, 2011)

Abstract

The document summarizes the present baseline of the target system for a 4-MW proton beam that is to product low-energy pions whose daughter muons are used in a Muon Collider or a Neutrino Factory. The target system consists of a free liquid mercury jet immersed in a high-field solenoid magnet capture system that also incorporates the proton beam dump.

1. Introduction to the Target System Baseline

The requirements for a Muon Collider/Neutrino Factory[1] (some of which are summarized in Table 1) call for a target capable of intercepting and surviving a 4-MW pulsed (15-50 Hz) proton beam.

Table 1. Baseline proton beam parameters.

Proton-beam energy	8 GeV
Rep rate (Neutrino Factory)	50 Hz
Rep rate (Muon Collider)	15 Hz
Bunch structure (Neutrino Factory)	3 bunches, 240 μsec total
Bunch structure (Muon Collider)	1 bunch
Bunch width	2 ± 1 ns
Beam radius	1.2 mm (rms)
Beam power	4 MW (3.125×10^{15} protons/sec)

A $\mu^+\mu^-$ collider requires simultaneous production/capture of charged pions, which mandates the use of solenoid magnets in the target system (rather than toroidal magnets that primarily capture particles of one sign, as is typical in target systems for "conventional" neutrino beams). In this document, it is taken as a requirement that the target system for a Muon Collide and that for a Neutrino Factory be essentially identical.

The target-system concept is illustrated in Fig. 1, in a version slightly modified from Neutrino Factory Study 2.[2] The target, the proton beam dump, and a shield/heat exchanger are to be located inside a channel of superconducting solenoid magnets that capture, confine and transport secondary pions and their decay muon, of energy 100-400 MeV, to the bunching, phase-rotation, cooling and acceleration sections downstream. Most of the 4-MW beam power is to be dissipated within a few meters, inside the solenoid channel, which presents a severe challenge. The present baseline target system included considerable more shielding of the superconducting magnet near the target, as sketched in the upper part of Fig. 2. See also Figs. 3 and 4. Studies of the tradeoffs between capital costs and operational costs including frequency of replacement of irradiated components are ongoing, and the baseline configuration is expected to evolve considerably in the near future.

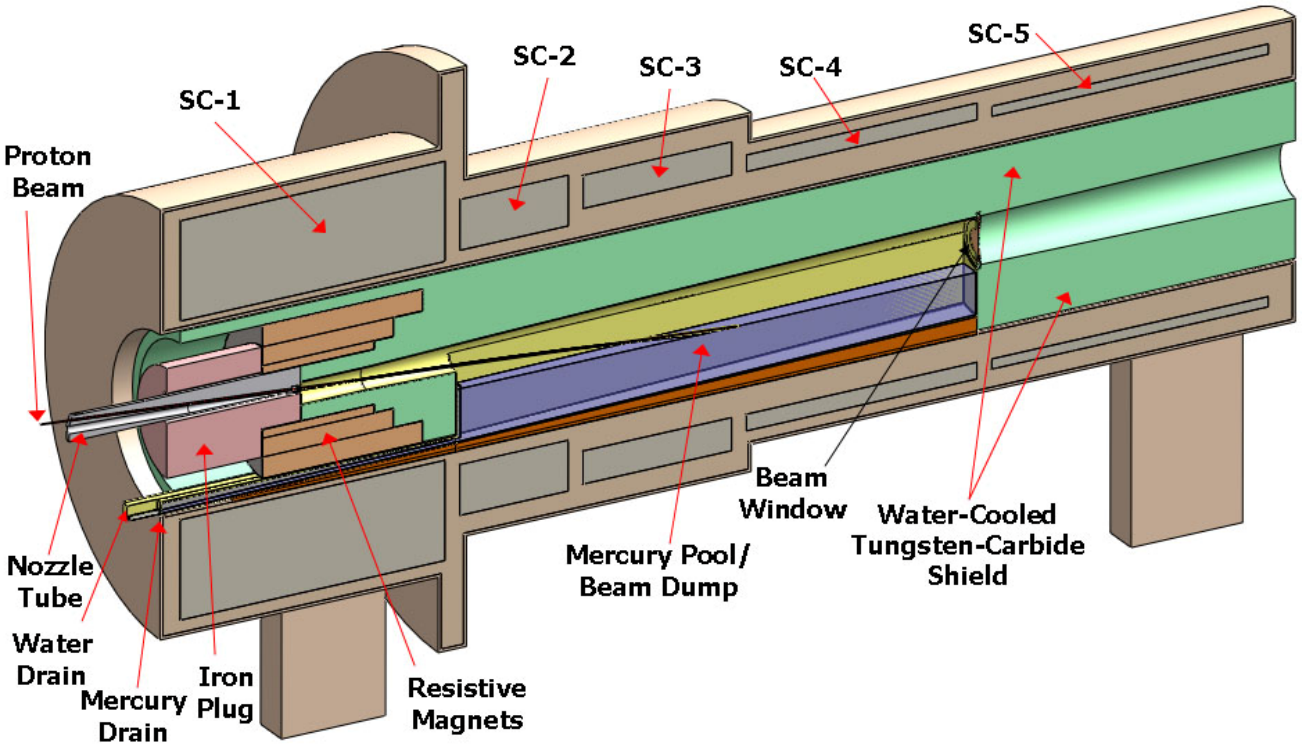

Fig. 1. Target-system concept, with small changes from Neutrino Factory Study II.[2]

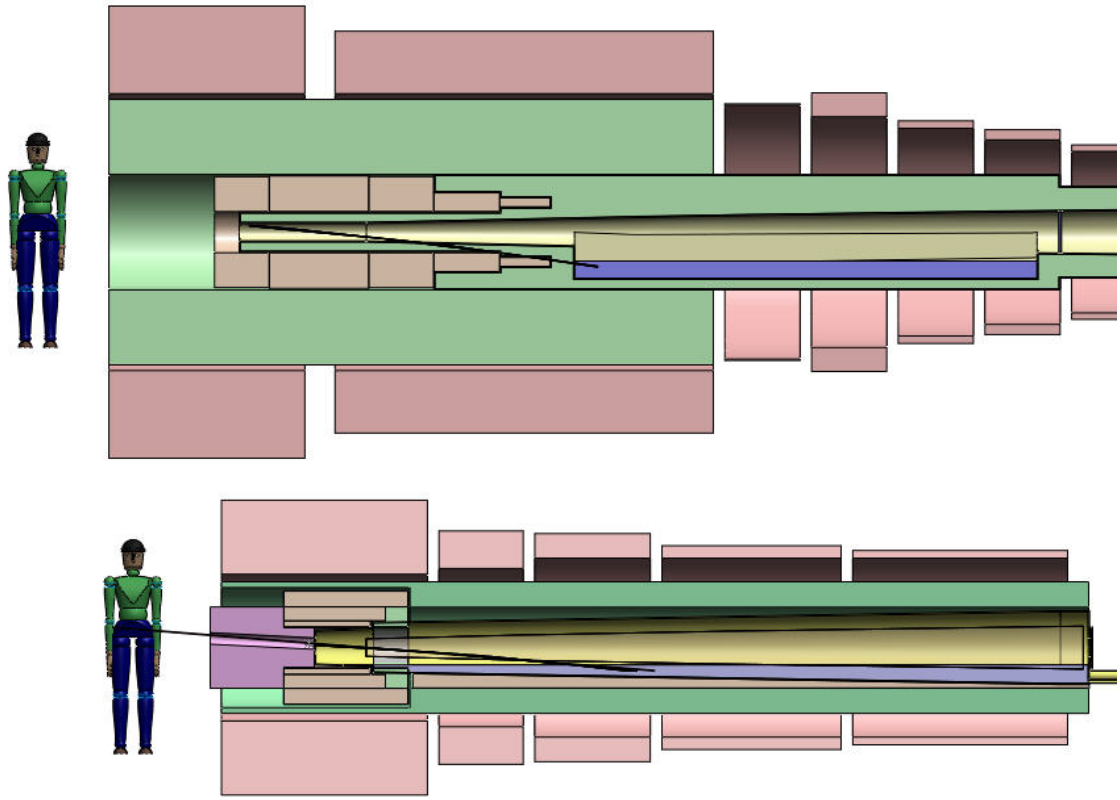

Fig. 2. Comparison of present vision of the target system (top) with that of Neutrino Factory Study II (bottom).

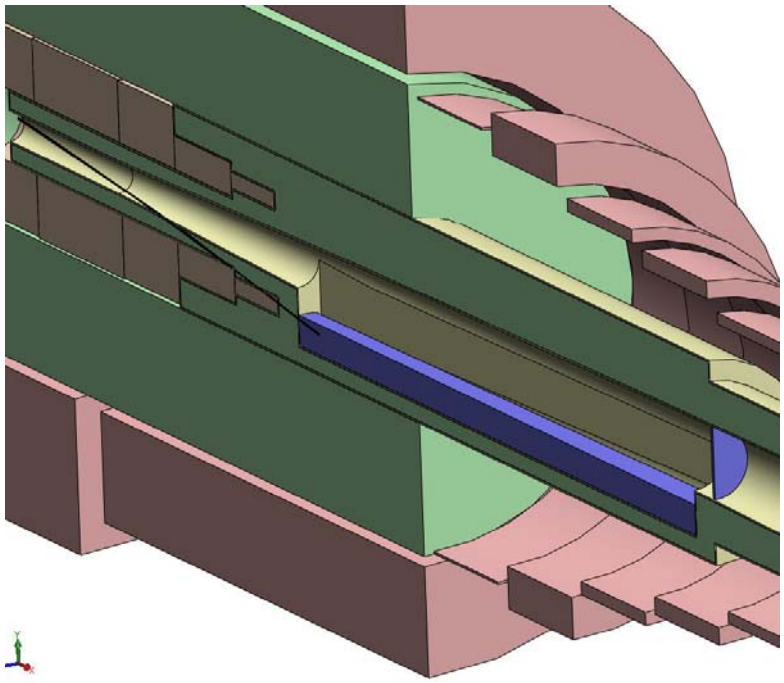

Fig. 3 Isometric view of the upstream region of the baseline target system, including the mercury collection pool/beam dump and the downstream beryllium window.

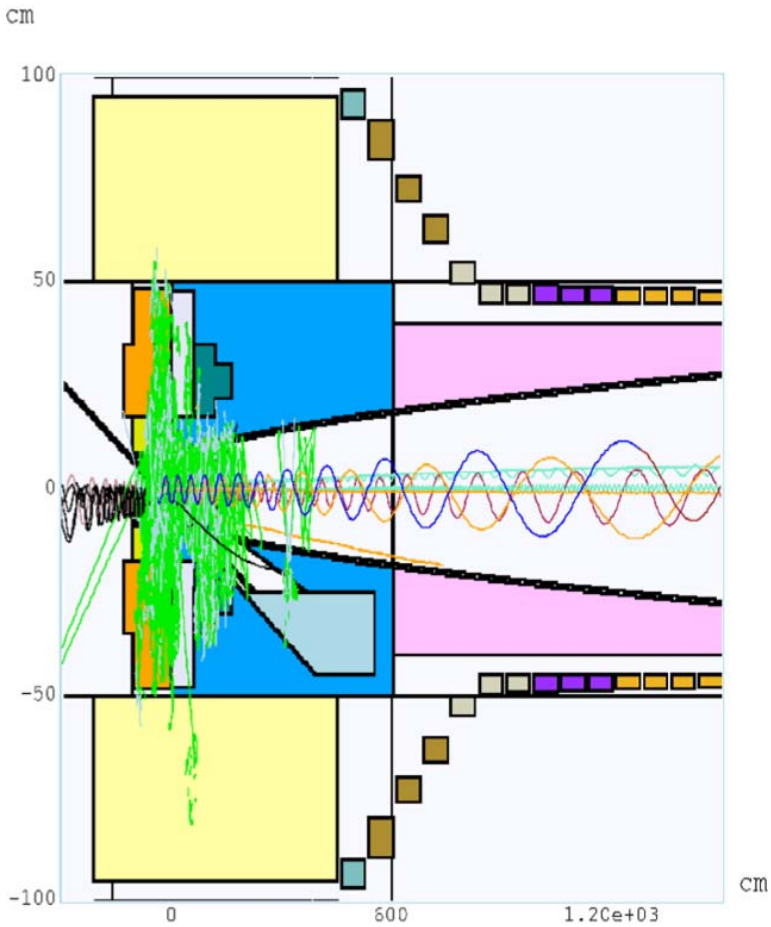

Fig. 4. MARS15 simulation of 9 proton interaction, showing 3 forward protons (one of which enters the shield), 5 forward pions, 5 backward soft protons, and various neutral particles.

Maximal production of low-energy pions is obtained with a proton beam of 1-2 mm (rms) radius and a target of radius 2.5 times this, such that the secondaries exit the side of the target rather than its end.[3] The resulting high density of energy deposition in the target makes it questionable whether any passive solid target could survive at 4-MW beam power. Schemes for a set of moving solid targets are not very compatible with the surrounding solenoid magnets. Hence, the baseline target concept is for a free liquid jet target,[*] in particular mercury. The present baseline parameters of the target are summarized in Table 2.

Table 2.Baseline target-system parameters

Target type	Free mercury jet
Jet diameter	8 mm
Jet velocity	20 m/s
Jet/solenoid-axis angle	96 mrad
Proton-beam/solenoid-axis angle	96 mrad
Proton-beam/jet angle	27 mrad
Capture solenoid field strength	20 T
Front-end π / μ transport channel field strength	1.5T
Length of transition between 20 T and 1.5 T	15 m

This target concept has been validated by R&D over the past decade, culminating in the so-called MERIT experiment[4] that ran in the Fall of 2007 at the CERN PS. The experiment benefited from the intensity of the beam pulses (up to 30 x 10^{12} *p*pp) and the flexible beam structure available for the extracted PS proton beam. Key experimental results include demonstration that:[5]

- The magnetic field of the solenoid greatly mitigates both the extent of the disruption of the mercury and the velocity of the ejected mercury after interception of the proton beam. The disruption of a 20-m/s mercury jet in a 20-T field is sufficiently limited that 70-Hz operational is feasible without loss of secondary particle production.
- Individual beam pulses with energies up to 115 kJ can be safely accommodated.
- Subsequent proton beam pulses separated by up to 350 μsec have the same efficiency for secondary particle production as does the initial pulse.
- Two beam pulses separated by more than 6 μsec disrupt the mercury independently.

The mercury jet is collected in a pool, inside the solenoid magnet channel, that also serves as the proton beam dump, as sketched in Fig. 1. Disruption of this pool by the mercury jet (whose mechanical power is 2.7 kW) and by the noninteracting part of the proton beam is nontrivial, and needs further study.

The superconducting magnets of the target system must be shielded against the heat and the radiation damage caused by secondary particles from the target (and beam dump). A high-density shield is favored to minimize the inner radii of the magnets. The baseline shield concept is for water-cooled

[*] The intense pressure waves in a liquid target due to a pulsed beam lead to damage/failure of any pipe that contains the liquid in the interaction region. Thus, the baseline is for a free liquid jet.

tungsten-carbide beads inside a stainless steel vessel (of complex shape, as sketched in Fig. 2).

The magnets of the target system vary in strength from 20 T down to 1.5 T in the subsequent constant-field transport channel,[†] with a corresponding increase in the radius of the capture channel from 7.5 cm to 30 cm.

A 20-T field is beyond the capability of Nb_3Sn, so the 20-T coil set is proposed as a hybrid of a 14-T superconducting coil outsert with a 6-T hollow-core copper solenoid insert. A 45-T solenoid of this type of construction has been operational since 2000 at the National High Magnetic Field Laboratory (Florida),[6] and a 19-T magnet of this type with 16-cm-diameter bore exists at the Grenoble High Magnetic Field Laboratory[7] (and was used in an earlier phase[8] of our R&D program). A topic for further study is possible fabrication of the 20-T magnet with high-T_C superconductor and no copper solenoid insert, which could provide more space for internal shielding of SC-1 and/or permit operation at a higher field for improved reduction of the initial beam emittance.

The target system (and also the subsequent π/μ solenoid transport channel) will be subject to considerable activation, such that once beam has arrived on target all subsequent maintenance must be performed by remote-handling equipment. The infrastructure associated with the target hall, with its remote-handling equipment, and hot-cells for eventual processing of activated materials, may be the dominant cost of the target system.

2 Subsystems

Section 2 presents details of the various subsystem of the target system, including an assessment of risks, possible mitigations, and alternate concepts.

2.1 Target

2.1.1 Baseline Concept

The target itself is a free liquid mercury jet ($Z = 80$, $A = 200.6$, density $\rho = 13.5$ g/cm^3, $\lambda_I \approx 15$ cm) of diameter $d = 8$ mm, flowing at $v = 20$ m/s. The volume flow rate is 1.0 l/s, and the mechanical power in the flowing jet is 2.7 kW. The flow speed of 20 m/s insures that the gravitational curvature of the jet over 2 interaction lengths (30 cm) is negligible compared to its diameter, and that more than 2 interaction lengths of new target material are present to the beam every cycle of 20 ms (at 50 Hz).

According to a MARS15[9] simulation,[3,10] about 11% of the beam energy is deposited in the target, corresponding to 9 kJ at 50 Hz. This energy is deposited roughly uniformly over 2 interaction lengths along the jet (30 cm, 15 cm^3), so the temperature rise of the mercury during a beam pulse is about 130K at 50 Hz and 440K at 15 Hz, noting that the specific heat of mercury is about 4.7 J/cm^3/K. The boiling point of mercury is 357°C, so the room-temperature mercury jet is vaporized at 15-Hz operation, but not at 50 Hz.

If the mercury jet is not vaporized, it will be disrupted and dispersed by the pressure waves induced by the pulsed energy deposition. The MERIT experiment[11] showed that for pulses equivalent to 50-Hz

[†] The target system is defined to end where the subsequent constant-field capture channel begins, at z =15 m downstream of the downstream end of the beam-jet interaction region ($z = 0$)..

operation at 4 MW beam power, this disruption results in droplets of peak velocity about 50 cm/s in 15-T field, with an extrapolation to a velocity of about 30 cm/s in 20 T, as shown in Fig. 3. If the target did not vaporize at 15-Hz operation, the peak droplet velocity is extrapolated to be about 100 cm/s, which raises an issued as to possible erosion of the stainless steel containment vessel.

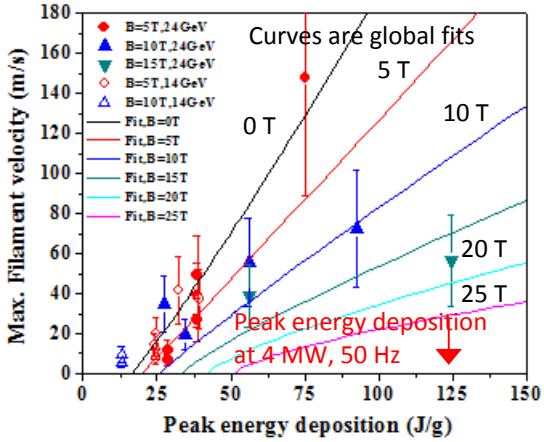

Fig. 3. Filament velocity vs. energy deposition as observed in the MERIT experiment.[11]

The optimal production of low-energy pions as usefully converted to muons and cooled and accelerated in the subsequent muon-beam complex is achieved by appropriate tilts of the mercury jet and proton beam with respect to the magnetic axis. These tilts depend slowly on the proton beam energy (as does the optimum radius of the jet), and the current best values (from a MARS15 simulation[3]) are given in Table 2.

The Reynolds number of the mercury flow in the jet is $R = \rho v d / \eta \approx 1400$, noting that the viscosity of mercury is $\eta = 1.5$ c.g.s. units, such that the flow is turbulent. Hence, the quality of the jet is an issue, although operation in a high magnetic field damps surface perturbations.[8] The nozzle will be as close as feasible to the interaction region; design of the nozzle is ongoing.

2.1.2 Risks, Mitigations, Alternatives

2.1.2.1 Release of Activated Mercury Vapor or Liquid Mercury due to Catastrophic Failure

It is hard to quantify this risk, which is associated with earthquakes, and terrorist attacks.

Mitigations include design of the target system for survival of earthquakes and terrorist attacks.

Alternatives include use of a liquid metal target that is solid at room temperature, such a eutectic alloy of lead and bismuth (melting point 124°C), or powder targets, or solid targets.

Use of a lead-bismuth target would lead to rather similar performance to a mercury target, with the challenge of operating the target flow loop at temperatures above the boiling point of water, with that flow loop in thermal contact with the water-cooled shield of the superconducting magnets. The activation products from a lead-bismuth target are somewhat more troublesome than those of mercury target.

The tungsten-powder target is being developed at RAL.[12] Recirculation of the powder within the very

tight confines of the target system is problematic, but perhaps not impossible. The lifetime of the pipe carrying the powder in the vicinity of the interaction point would be very short due to radiation damage, such that frequent replacement of this part of the system would be required, and cooling of this pipe is problematic.

A solid graphite target, radiation cooled, was considered for use at 1-MW beam power in Neutrino Factory Feasibility Study I. This results in slightly lower pion yields per proton, and requires magnet SC-1 to be longer, as the interaction length of graphite is about 85 cm. Frequent replacements (every 2-4 weeks) of such a target would be required to avoid mechanical failure induced by radiation damage.

At present, no effort is being made within the Muon Accelerator Program on these alternatives.

2.1.2.2 The Beam-Jet Interaction Is More Destructive Than Anticipated

While the MERIT experiment indicates that the disruption of the mercury jet by the proton beam is not destructive of the containment vessel,[5] this result is from a study of only a few pulses. The velocity of the dispersed droplets appears to scale roughly linearly with proton flux (particles/area), and roughly inversely with the magnetic field in which the target is immersed.

This issue would be mitigated by use of higher magnetic field on the target (which also could have the effect of improved pion yield, in exchange for use a higher risk magnet), and by reduced proton beam intensity (and consequent reduction in pion yield).

Our understanding of this issue would be improved by a repeat of the MERIT experiment, for greater numbers of pulses, and by continued numerical modeling. The former is considered impractical for the present, while the latter is being pursued by R. Samulyak of SUNY Stony Brook. He and his team use the so-called FronTier code to address this challenging problem,[13] with increasingly sophisticated results. An example is shown in Fig. 2 of how high magnetic fields suppress the disruptions of a mercury jet. Effort is ongoing to simulate one of the subtler effects of the mercury-beam interaction, the apparent (transient) reduction in the speed of sound within the mercury after a beam pulse.

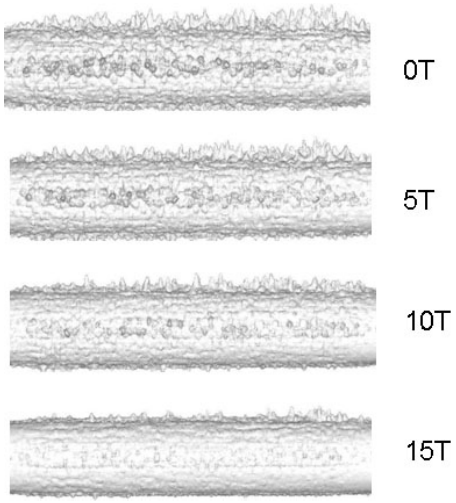

Fig. 2. FronTier simulation of the suppression by high magnetic field of filamentation of a mercury jet.[13]

2.1.2.3 The Jet Quality Is Poorer Than Anticipated

The quality of the 1-cm-diameter mercury jet at 15-20 m/s velocity in the MERIT experiment was rather poor.[5] The effect of this on the pion yield was hard to assess, and may not have been too serious.

Clearly, it would be better to have a better quality jet, based on a program of theoretical and numerical investigation, followed by possible validation in experiments (at zero magnetic field).

Such a program has recently begun, led by F. Ladiende of SUNY Stony Brook. It is too early to report results of this effort, other than a conjecture that cavitation inside the nozzle may have been the cause of the poor jet quality, as has been observed elsewhere in high-Reynolds-number flow.[14]

2.1.2.4 **The Pion Yield is Not Optimal**

Many factors influence the pion production in the target: proton beam energy, target material, target radius, target length, target and beam angles with respect to the magnetic axis, as well as the acceptance of the downstream systems of the Muon Collider/Neutrino Factory. If/when these parameters and requirements change, the target parameters should be re-optimized. Simulations of pion production at the target station of a Muon Collider have been performed using the MARS code[9] since at least 1997,[15] and need to be continued with greater sophistication so as to optimize the various relevant parameters. In addition, the MARS15 code should be verified for our application by comparison with calculations using FLUKA.

The simulations of particle production in the target system rely on extrapolation from experimental data that unfortunately have various inconsistencies in the relevant regions of parameter space.[16] Assessment of the seriousness of this issue is ongoing, but it may well be desirable to collect additional data relevant to particle production at a Muon Collider/Neutrino Factory. The Fermilab MIPP experiment upgrade (P-960)[17] affords an opportunity for such studies.

2.2 **Proton Beam Dump**

2.2.1 Baseline Concept

The target system of the Muon Collider/Neutrino Factory target system requires the proton beam dump to be inside the superconducting magnet channel, only ≈ 1 m from the target. The baseline design is to use the pool that collects the mercury from the target jet as the beam dump. The mercury is to be drained from downstream end of the pool (close to the outlet of the water flow for the inner, upstream tungsten-carbide shield).

The dump must dissipate the roughly 3 kW of mechanical power in the mercury jet, as well as roughly 20 kW of power in the attenuated proton beam.

The vessel that contains the mercury pool will be subject to substantial radiation damage and heating by the secondary particle from the target, and must be replaceable. This vessel may need to be the same as the inner surface of the internal shield (sec. 2.4) as water cooling is foreseen for the latter.

2.2.2 Risks, Mitigations, Alternatives

2.2.2.1 Mercury Flow Fails and Full Proton Beam Strikes the Dump

If the target flow were to fail and the full proton beam delivered onto the beam dump, roughly 15% of the beam energy would be dissipated in the dump, 30 times nominal (and the peak energy deposition in the surrounding shield and superconducting magnets would be many times nominal). It will not be

possible to have direct verification of the presence of the target, but indirect checks of the mercury flow rate into and out of the target system can provide an interlock for the beam permit.

An option that could further mitigate this risk is use of a solid graphite "post target" in the (limited) space downstream of the interaction region, and above the surface of the dump pool, where the jet has separated from the beam. Such a "post target" would dissipate about 20 kW of power, and could have a lifetime against radiation damage of more than one year. No study of this option has been made yet.

2.2.2.2 The Perturbations of the Dump Pool by the Beam and Jet are Excessive

The mercury pool is subject to perturbation by the jet and by the attenuated proton beam.[18] The perturbations, a simulation of which is shown in Fig. 3, are to be damped by a set of baffles or absorbers for which there is no design at present.

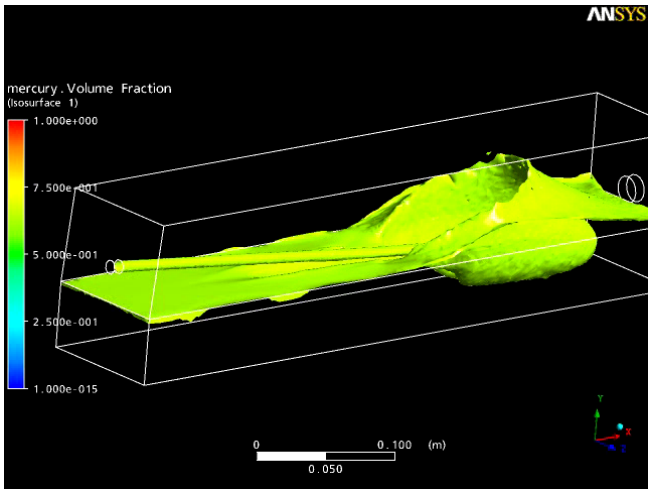

Fig. 3. ANSYS simulation of a mercury jet entering a mercury pool.[18]

2.2.2.3 The Flow Rate Out of the Pool is Insufficient

If the flow rate out of the pool were insufficient the target chamber would fill with mercury and become useless. This risk can be mitigated by hydraulic engineering studies, not yet performed, but it may be prudent to validate the eventual design with a full-scale laboratory test of the flow in the pool (and of the "splash mitigator" of item 2.2.2.2).

2.2.2.4 The Cooling of the Mercury Containment Vessel is Insufficient

The energy deposition in the mercury containment vessel, due to secondary particles from the target, will be several hundred kW, but no scheme for cooling this vessel (if separate from the internal shiled) has been considered to date.

2.2.2.5 The Mercury Containment Vessel Fails Due to Radiation Damage

This risk is to be mitigated by replacement of the entire vessel at appropriate intervals, not yet defined. It is anticipated that the downstream beam window (sec. 2.3), the internal magnet shield (sec. 2.4), and the resistive magnet insert (sec. 2.5) will be replaced at the same time as the mercury containment vessel.

2.2.2.6 No Satisfactory Solution Is Found for a Liquid-Metal Beam Dump

If no satisfactory solution is found for a liquid metal beam dump, an alternative would be a solid target, followed by a solid beam dump. In this scenario, the target would have to be replaced frequently, such that less frequent replacement of the solid beam dump would be only a modest additional operational burden. This option is not under study at present.

2.3 Beam Windows

2.3.1 Baseline Concept

The volume that contains the target and mercury pool beam dump is the primary containment vessel for the mercury. This containment vessel includes a small window somewhere upstream through which the proton beam enters, and a larger window on the downstream face of the vessel, specified to be at the boundary between superconducting magnets SC-7 and SC-8 (z = 6 m), through which the desired secondary protons (as well as other particles) pass. The containment vessel is to be operated with helium gas (plus mercury vapor) at atmospheric pressure.

The proton beam window has never been specified, either as to design or location, as this has been considered a relatively minor issue, addressable at some later time.

The larger exit window is specified as made of beryllium. It will be a double window, such that the volume between the two windows can support a flow of helium gas for cooling the window, and which can be monitored for indications of window failure.[19] The window system is a replaceable item, and will be sealed to the downstream face of the primary containment vessel and to the upstream face of the pion-decay-channel vessel via inflatable "pillow" seals. At present, it is not specified whether the beryllium window is to be installed/replaced via vertical or by axial access.

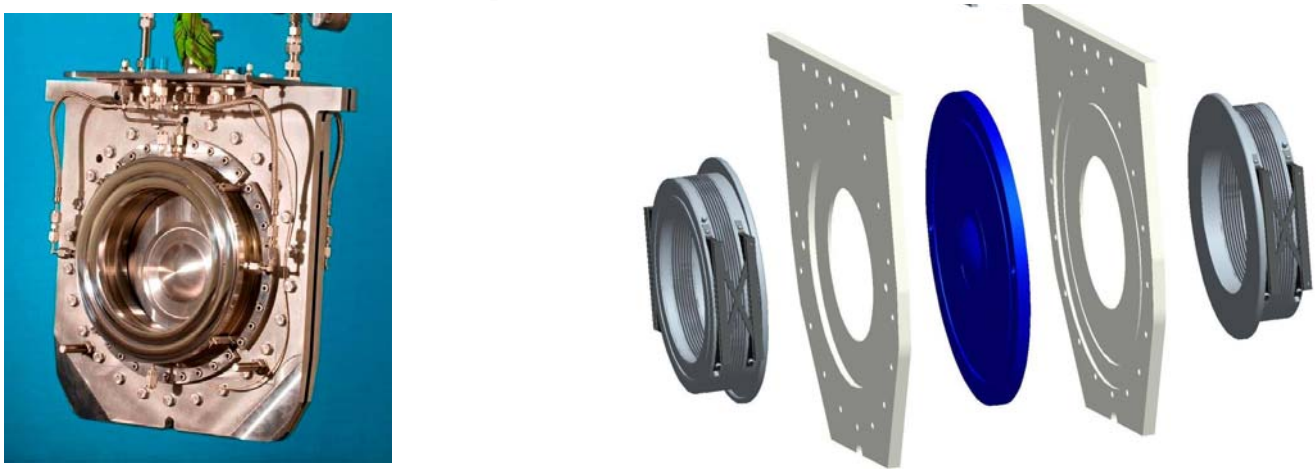

Fig. 4. Photograph and schematic of the T2K beam window.[19]

2.3.2 Risks, Mitigations, Alternatives

2.3.2.1 Failure of the Upstream Beam Window

This window should be designed not to fail. No design work has been performed to date.

2.3.2.2 **Failure of the Downstream Beam Window**

This window should be designed not to fail. No design work has been performed to date.

The risk of failure of the downstream beam window would be reduced if the pion-decay channel (downstream of it) were operated at atmospheric pressure (and the beam window that makes the transition to vacuum be located farther downstream in a less demanding environment). An alternative which is also favorable in this respect is that the pion-decay channel begin with a solid absorbed to which the beam window is sealed. The absorber could serve to attenuate the flux of protons in pion-decay channel, to reshape the pion spectrum, and to provide transverse emittance cooling (if made of a sufficiently low-Z material.[20]

2.4 Pion Decay Channel

2.4.1 Baseline Concept

The pion decay channel is the volume inside the beam pipe (that serves as the inner surface of the internal shield (sec. 2.5), which volume extends well past z = 15 m which is the nominal end of the target system. The mercury containment vessel at z < 6 m is part of the pion decay channel. It would be appropriate that the pion decay channel for z > 6 m be at atmospheric pressure of He gas (or H2 gas) to minimize stresses on the beryllium window at z = 6 m.

2.4.2 Risks, Mitigations, Alternatives

2.5 **The Internal Shield**

2.5.1 Baseline Concept

A major challenge of the target system is the dissipation of the 4-MW of beam power inside the superconducting magnet string without quenching of the magnets, or extreme shortening of the operational lives due to radiation damage. Most of the beam power will be dissipated in an internal shield of a high-Z material, which will have to extend well beyond the target system in the front end.

The baseline scenario is for a shield of tungsten-carbide beads cooled by water. Pure tungsten beads would provide better shielding, but tungsten corrodes in water in a high radiation environment.[21] Random packing of spherical beads of a single radius will result in a configuration with about 63% by volume of tungsten-carbide, and 36% water.[22] The flow path of the coolant is not presently specified; multiple inlets and outlets will be appropriate for a shield of total length 30-50 m, with one inlet at the very upstream end of the shield where the heat load is the largest.

The outer radius of the shield was specified as 63 cm in Feasibility Study II,[2] but subsequent MARS15 simulations (with MCNP additions) indicated that this would imply a load of ≈ 38 kW in magnet SC-1 of that configuration.[3] To reduce the thermal load on and radiation damage to the magnets an interim value of r = 120 cm been adopted for the inner radius of the superconducting magnets near the target, and the outer radius of the shield increased to 115 cm. Studies are ongoing to clarify criteria as to acceptable total power deposition, and peak local power deposition, for the various magnets (of various designs) to be stable against quenching and radiation damage. See also sec. 2.6.1. The present baseline concept is only preliminary.

2.5.2 **Risks, Mitigations, Alternatives**

The risk that the baseline shield will not perform adequately is high because of insufficient study of the issues, which are related to magnet design as well as to that of the shield itself. Once the shield is built it is too late to modify it. All mitigation of risks must be done in the design.

2.5.2.1 **The Shielding Against Pulsed Thermal Loads is Insufficient**

Reliable operation of superconducting magnets requires the temperature rise during a single beam pulse to be ≤ 1K (assuming that the magnet cooling is sufficient to reduce the temperature to nominal before the next beam pulse). This leads to a requirement that the peak energy deposition per beam pulse be ≤ 0.1 mJ/g, and hence a peak power deposition of ≤ 5 mJ/g at 50-Hz operation.

The baseline scenario for the internal shield of the superconducting magnets is a vessel filled with tungsten-carbide spheres, cooled by water flow. As the geometry of the internal shield is complex, it is not evident that sufficient uniformity of the water flow can be achieved to avoid regions in which there is only steam rather than water, which could then lead to local melting of the shield wall. To address this issue, and to consider alternatives with, say, tantalum shielding with long channels for the coolant, or shielding with mercury, simulations of heat transfer in complex geometries are required.

We are presently exploring the prospect of such simulation with the Peles group at RPI.[23]

An alternative that would provide greater shielding for a given thickness is to use mercury rather than tungsten-carbide/water.[24] A variant on this alternative is to use tungsten-carbide beads cooled by mercury, or lead-bismuth eutectic liquid, as the coolant.

2.5.2.2 **The Shielding Against the Average Thermal Load is Insufficient**

The maximum average thermal load which permits viable operation of the superconducting magnets is an issue of the design of the magnet cooling, and of the cooling plant at 4K. At present there is no crisp statement as to the maximum average thermal load, so the design process of the shield is at risk for lack of this information.

2.5.2.3 **The Shielding Against Radiation Damage to the Magnets is Insufficient**

The baseline design follows the specification of the ITER project that the cable-in-conduit superconductor be subject to less than 1 mW/cm^3 (0.17 mW/g for conductor of specific gravity 6) of energy deposition due to penetrating particles if a lifetime of 10 years (of 10^7 s each) is desired.[25] MARS15 simulations of various thicknesses of tungsten-carbide shields at (z < 6 m) have been performed, with results illustrated in Figs. 5 and 6. These preliminary studies suggests that if the inner, resistive magnets are as compact as sketched, then a configuration (so-called IDS90f) with 90-cm inner radius of the first three superconducting magnets would be sufficient for a 10 year lifetime of those magnets. However, electrical and cooling services for the resistive magnets will very likely occupy a substantial volume (not shown), such that we take the present baseline configuration to be the IDS120f scenario.

The peak energy deposition in mW/g in magnet SC3 (see sec. 2.6) for operation at 4-MW beam power is

plotted as a function of its inner radius in Fig. 7 (left), and the total thermal load on all 19 of the target-system superconducting magnets is shown in Fig. 7 (right). The advantage, say, of a 20-year magnet lifetime and lower operational cost or removal of kW thermal power at 4K is to be contrasted with the increased capital cost of a configuration with larger internal radius, such as the baseline IDS120f.

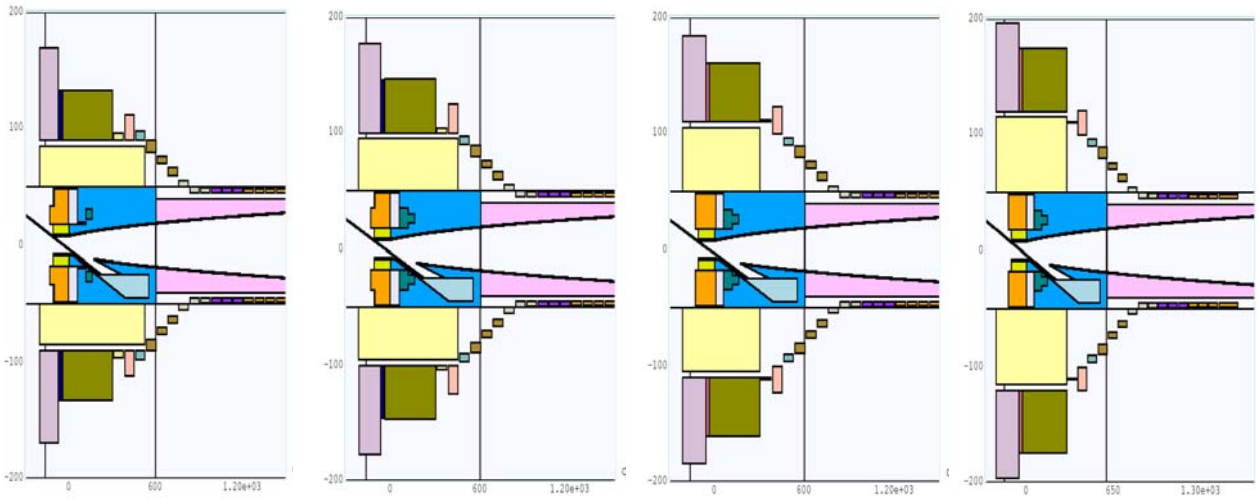

Fig. 6. Sketches of magnet/shielding configurations IDS90f, IDS100f, IDS110f and IDS120f.

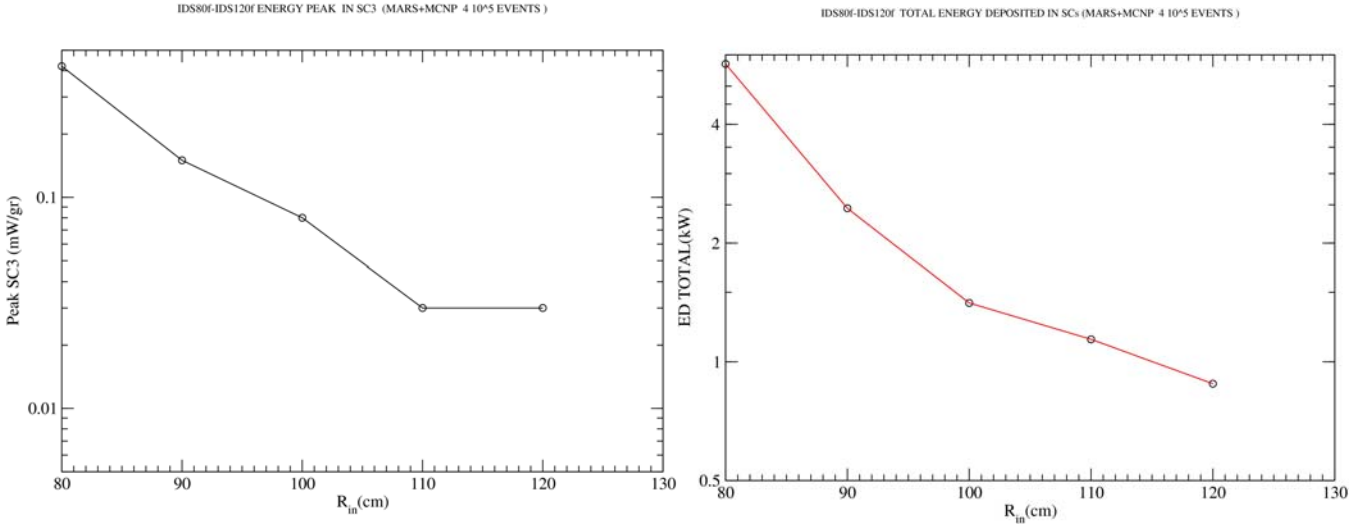

Fig. 7. Peak energy deposition in magnet SC3 (left), and total thermal power load due to particle energy deposition in superconducting magnets 1-19, as a function of inner radius of magnets SC1-3, for operation at 4 MW proton beam power.

2.5.2.4 **The Cooling of the Shield is Insufficient to Prevent It from Melting**

The location and size of possible coolant inlets and outlets is intertwined with issues of mechanical support of the intermagnet forces. The shield performance is at risk because no study of these issues, which would require a mix of cryogenic magnet engineering and room-temperature hydraulic engineering, has been performed. It may be prudent to build a full scale mockup of the shield to verify that the coolant flow rate is sufficient throughout to prevent local hot spots.

An alternative is to use a high-*Z* liquid metal, such as mercury, or lead-bismuth eutectic, as the shield

material.

2.5.2.5 **The Cooling of the Shield Containment Vessel is Insufficient to Prevent It from Melting**

MARS15 simulations suggest that the stainless-steel vessel that contains the tungsten-carbide beads will dissipate 500 kW of power (as much as the target itself). The containment vessel is at risk because no study of these issues has been performed.

2.5.2.6 **The Containment Vessel of the Shield Fails Due to Radiation Damage or Erosion by Mercury Droplets**

This risk can be mitigated by replacement of the shield and containment vessel at appropriate intervals, which have not yet been identified. The risk of erosion due to mercury droplets can be mitigated by operation of magnet SC1 at a higher field.

2.5.2.7 **The Containment Vessel Deforms Such that It Cannot Be Removed for Replacement**

The mass of the tungsten-carbide of the shielding is roughly 100 tons, which must be supported by the cryostats of the superconducting magnets of the target system. To the extent that the tungsten-carbide beads plus coolant water behave like a liquid, substantial deformations of their containment vessels are to be anticipated, as illustrated in Fig. 8. No engineering studies as to mitigation of this issue have been performed.

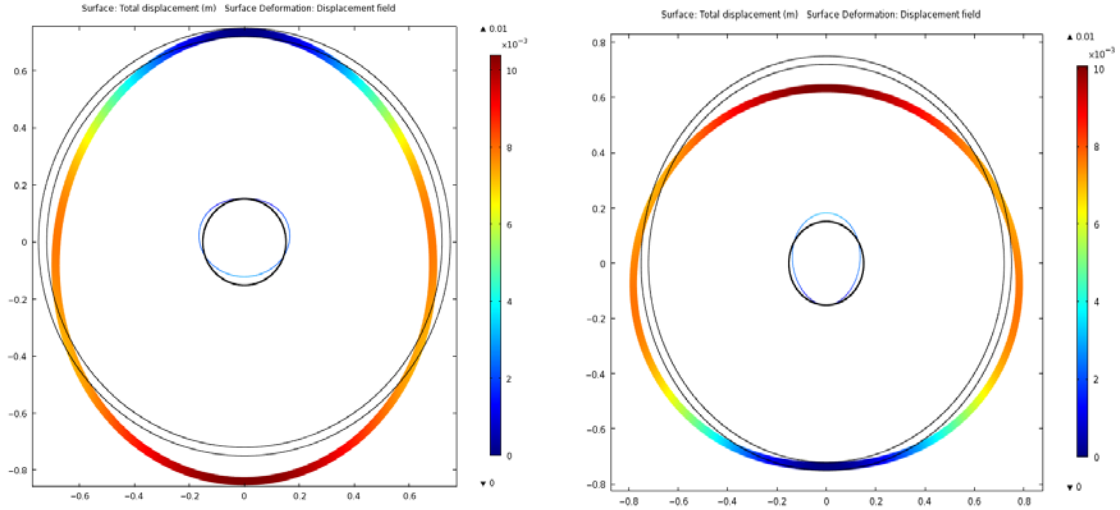

Fig. 8. Model calculations of deformations of the containment vessel of the tungsten-carbide beads, assuming the latter behave like a liquid, and that possible stiffening rings are omitted. Deformations are magnified × 10, and are of order 2 mm.

2.6 The Solenoid Magnet String

2.6.1 Baseline Concept

An early concept[26] for a $\mu^+\mu^-$ collider assumed separate targets for production/collection of positive and negative particles. It was soon realized that use of solenoid magnets would permit a single channel to operate with both signs,[27] that initial capture in a high-field solenoid followed by solenoids of adiabatically lower fields exchanges transverse for longitudinal momentum,[28] and that solenoid magnet

coils would be farther (than toroidal coils) from the high radiation associated with the secondary particles from the target.[29]

The design of the first coil set, with baseline field of 20 T is particularly challenging. The use of a 6-T water-cooled, hollow core copper solenoid insert is required if the superconducting outsert is to be made from Nb_3Sn. This copper magnet receives a very high radiation dose (while acting as a partial shield of the superconducting outsert) and is anticipated to be a replaceable component with a lifetime of 4 years or less.[‡] These resistive magnets will dissipate about 12 MW, which power must be removed by water cooling (not presently designed). If the entire 20-T magnet were of this technology, the power dissipation would be about 300 MW.

Another issue is the very large axial forces between the various magnets of the target system. A further complication is the requirement that the axial field profile in the beam-jet interaction region be smooth, such that the mercury jet is minimally perturbed as it enters this field. The Study II scenario[2] called for an iron plug at the upstream end of the first magnet, through which the proton beam and mercury jet would enter. The presence of this plug would add considerable complexity to the mechanical design of the system, and has been eliminated from the present baseline.

The present baseline magnet parameters (so-called IDS120f) are given in Table 3, and a longitudinal section of the magnet string in shown in Fig. 8. The axial field profile is shown in Fig. 9, whose taper is meant to follow the inverse-cubic form suggested by K. Paul,[30]

$$B_z(0, 0 < z < z_1) = \frac{B_0}{1 + a_2 z^2 + a_3 z^3}, \text{ where } \quad a_2 = 3\frac{B_0 / B_1 - 1}{z_1^2}, \quad a_3 = -2\frac{B_0 / B_1 - 1}{z_1^3}, \text{ with } \quad B_0 = 20\,\text{T},$$

$B_1 = 1.5\,\text{T}$, $z_1 = 15\,\text{m}$, and slopes $dB_z(0)/dz = dB_z(z_1)/dz = 0$.

Magnets RC1-5 are a nested set of water-cooled, hollow-core copper coils insulated with MgO (as shown in Fig. 9) for longer life in the high-radiation environment. These magnets are inside the superconducting coils SC1-3. The parameters of these magnets are chosen to provide an axial field flat to 1% over the target region, $-75\,\text{cm} < z < 0$, and with hoop stresses everywhere less than 400 MPa. All superconducting magnets will be fabricated using cable-in-conduit conductor, as used for the ITER magnet (Fig. 10).

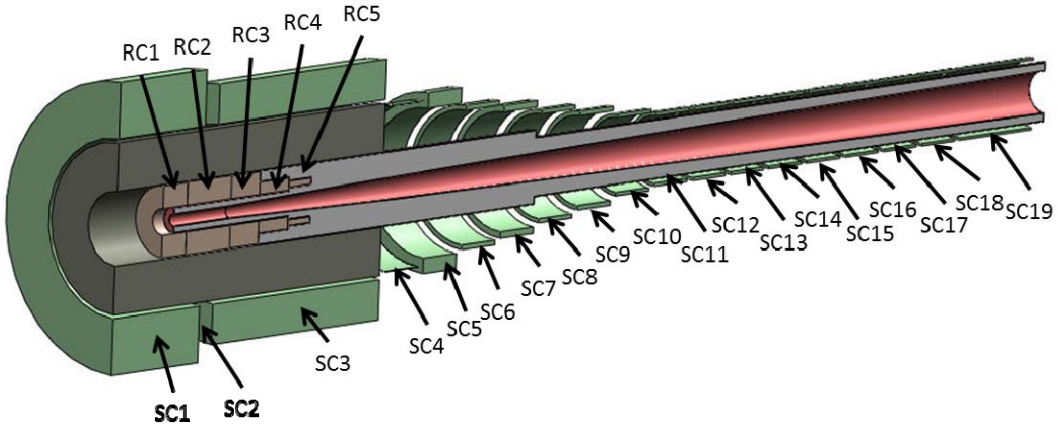

Fig. 8. Longitudinal section of the magnet string. RC = resistive conductor; SC = superconductor.

[‡] If the presence of this copper magnet leads to a requirement for thicker shielding and consequent larger inner diameter the superconducting outsert, such that the latter is untenable, we must consider the option of only a 14-T Nb_3Sn magnet, or development of a large-bore high-T_C magnet (or more simply, a high-T_C-Nb_3Sn hybrid;[‡] tests of YBCO indicate that it has good resistance to radiation damage[‡]).

Table 3. Baseline magnet parameters (IDS120f).

Magnet	z_{min} (cm)	Δz (cm)	r_{min} (cm)	Δr (cm)	I (A/mm^2)	Conductor
RC1	-131.3	47.3	17.8	30.24	16.56	Cu
RC2	-84	86.2	17.8	30.88	16.56	Cu
RC3	2.1	56.2	17.8	30.25	16.56	Cu
RC4	58.3	57	17.8	16.6	16.56	Cu
RC5	115.3	43.5	21.88	7.96	16.56	Cu
SC1	-222.6	169.4	120	75.85	23.22	Nb3Sn
SC2	-53.1	26.1	120	54	0	Nb3Sn
SC3	-27.1	327.1	120	54.07	23.1	Nb3Sn
SC4	310	65	110	1.16	29.96	Nb3Sn
SC5	385	65	100	20.76	33.31	Nb3Sn
SC6	460	65	90	6.4	35.85	Nb3Sn
SC7	535	65	80	8.71	38.21	Nb3Sn
SC8	610	65	70	5.61	40	Nb3Sn
SC9	685	65	60	6.06	40	Nb3Sn
SC10	760	65	50	4.72	40	NbTi
SC11	835	65	45	4.6	40	NbTi
SC12	910	65	45	4.42	40	NbTi
SC13	985	65	45	4.31	40	NbTi
SC14	1060	65	45	3.85	40	NbTi
SC15	1135	65	45	3.83	40	NbTi
SC16	1210	65	45	3.51	40	NbTi
SC17	1285	65	45	3.53	40	NbTi
SC18	1360	65	45	3.44	40	NbTi
SC19	1435	140	45	3.24	40	NbTi

2.6.2 Risks, Mitigations, Alternatives

2.6.2.1Magnet Failure during a Quench

The stored energy in the 20-T magnet (coils SC1-3) is roughly 3 GJ. Dissipation of this large stored energy without damage to the magnet during a quench will require a very conservative design. Figure 11 shows the variation of stored magnetic energy with inner radius *r* of SC1-3, normalized to the energy of 1.3 GJ for $r = 80$ cm.

2.6.2.2 Magnet Quench Due to Energy Deposition by Secondary Particles from the Target

This risk must be avoided by sufficient internal shielding of the magnets (sec. 2.4), together with a robust design of the 4K liquid helium coolant system.

2.6.2.3 Magnet Failure Due to Radiation Damage

Electrical failure of the conductor insulation is more likely than mechanical failure of the conductor itself. This risk must be mitigated by use of radiation-hard insulators, and eventual replacement of magnets after accumulation of a specified radiation dose.

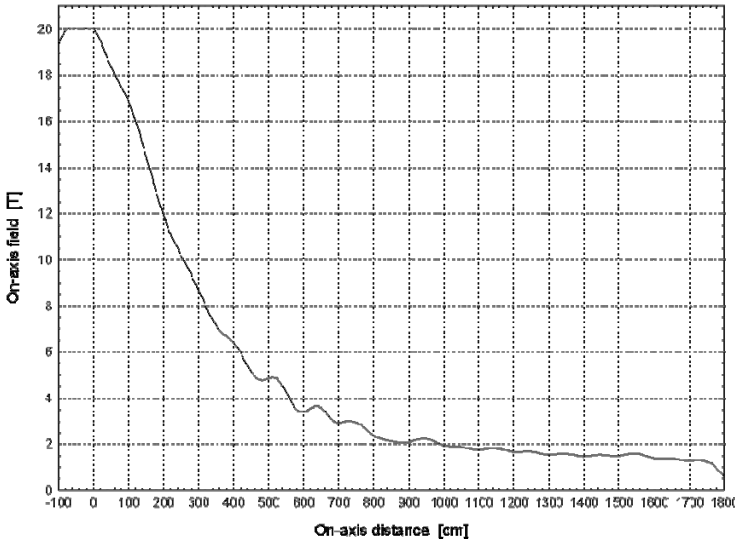

Fig. 8. Axial profile of the target magnet string.

Fig. 9. Mineral-insulated hollow conductor developed for Japan Hadron Facility.[31] The end-on view shows the white layer of powdered MgO insulation sandwiched between the copper hollow conductor and its sheath, also of copper. The conductor is 18 mm square with a 10~mm square cooling hole. The MgO is 1.8~mm thick, and the outer copper sheath, 1.1 mm, for an overall dimension of 23.8 mm. Of the cross section, 17% is cooling passage, 37% conductor, 28% insulation and 18% sheath. The side view shows a conductor termination, brazed of several parts that confine the MgO and hold the glossy white ceramic ring that keeps the sheath isolated from the current-carrying conductor.

The baseline design follows the specification of the ITER project that the cable-in-conduit supercnductor be subject to less than 1 mW/cm^3 (0.17 mW/g for a conductor of specific gravity 6) of energy deposition due to penetrating particles, if a lifetime of 10 years (of 10^7 s each) is desired.[32]

A conductor that can dissipate a heat load of 1 mW/cm^3 has been designed for ITER, and the target system baseline assumes use of this. A conductor could be designed with larger LHe coolant passages that could dissipate, say 2 mW/cm^3, thereby permitting a 5-year lifetime in a higher radiation environment associated with less internal shielding of the magnet.

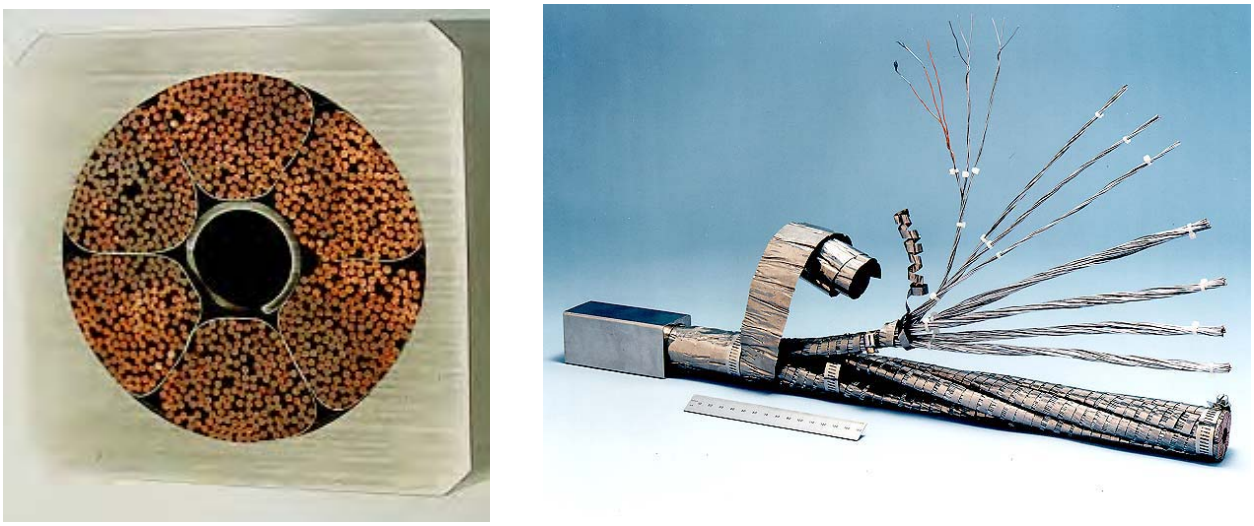

Fig. 10. ITER cable-in-conduit conductor.

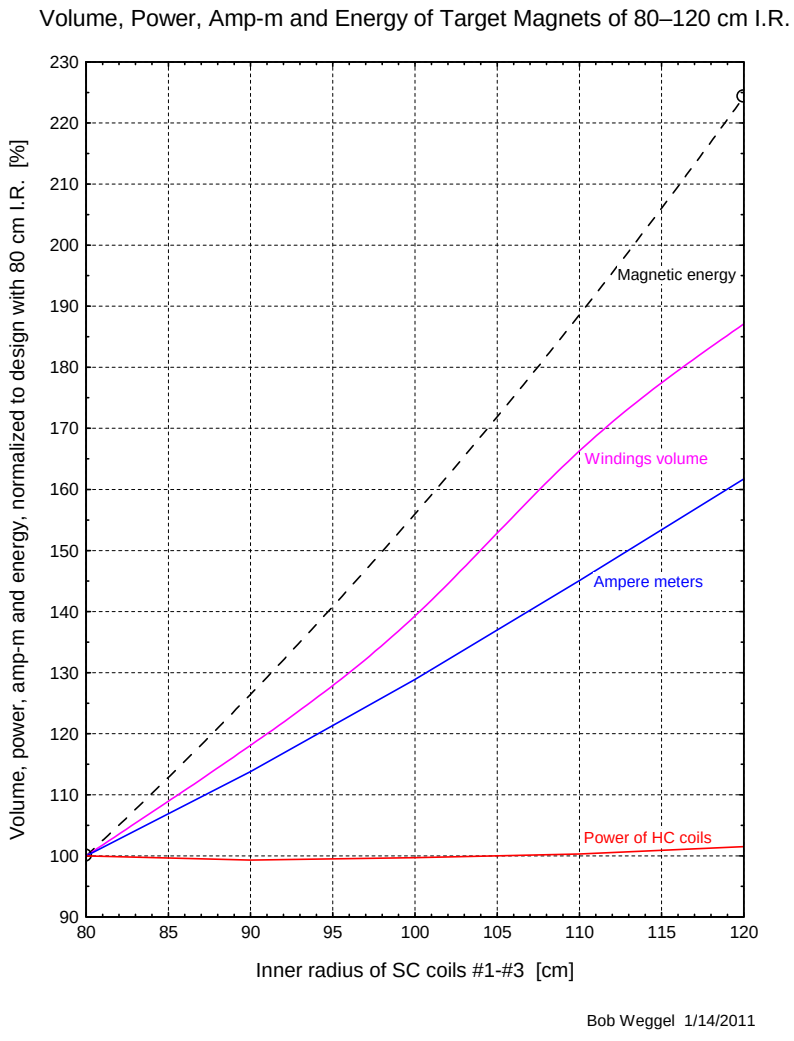

Fig. 11. Magnetic energy, winding mass/volume and Amp-m of superconducting coils SC1-3 as a function of their inner radius, normalized to the values of 1.3 GJ energy, 200 tons, and 54 MA-m at r = 80 cm.

2.7 Mercury Flow Loop

As the opportunity approaches to build a target system for a Muon Collider or Neutrino Factory, substantial effort will be needed on the engineering of infrastructure issues such as the mercury flow loop, the remote handling systems for maintenance, and the target hall. No work has been done on these issues since Neutrino Factory Study II,[2] which provides a basic vision of these subsystems.

2.7.1 Baseline Concept

2.7.2 Risks, Mitigations, Alternatives

2.8 Remote Handling Maintenance Systems

2.8.1 Baseline Concept

2.8.2 Risks, Mitigations, Alternatives

2.9 Target Hall

2.9.1 Baseline Concept

2.9.2 Risks, Mitigations, Alternatives

References

[1] M.M. Alsharo'a *et al., Status of Neutrino Factory and Muon Collider Research and Development and Future Plans*, Phys. Rev. ST Accel. Beams **6**, 081001 (2003), http://puhep1.princeton.edu/~mcdonald/examples/accel/alsharoa_prstab_6_081001_03.pdf

[2] S. Ozaki *et al*., *Feasibility Study II of a Muon-Based Neutrino Source* (June 14, 2001), http://www.cap.bnl.gov/mumu/studyii/FS2-report.html

[3] X. Ding *et al., A Pion Production and Capture System for a 4 MW Target Station*, IPAC10, http://www.hep.princeton.edu/~mcdonald/mumu/target/ipac10/thpec092.pdf

[4] J.R.J. Bennett *et al., Studies of a Target System for a 4-MW, 24-GeV Proton Beam, proposal to the ISOLDE and Neutron Time-of-Flight Experiments Committee*, CERN-INTC-P-186 (April 26, 2004), http://www.hep.princeton.edu/~mcdonald/mumu/target/cern_proposal.pdf

[5] K.T. McDonald *et al., The MERIT High-Power Target Experiment at the CERN PS*, PAC09, http://www.hep.princeton.edu/~mcdonald/mumu/target/pac09/tu4gri03.pdf

[6] 45-T Hybrid, NHMFL, http://www.magnet.fsu.edu/mediacenter/features/meetthemagnets/hybrid.html

[7] Magnet M8, GHMFL, http://ghmfl.grenoble.cnrs.fr/spip.php?rubrique77&lang=en

[8] A. Fabich, *High Power Proton Beam Shocks and Magnetohydrodynamics in a Mercury Jet Target for a Neutrino Factory,* Ph.D. thesis (U. Vienna, Nov. 2002), http://www.hep.princeton.edu/~mcdonald/mumu/target/thesis-2002-038.pdf

[9] The MARS Code System: http://www-ap.fnal.gov/MARS/

[10] X. Ding, *Energy Deposition of 4-MW Beam Power in a Mercury Jet Target* (Feb.9,2010), http://www.hep.princeton.edu/~mcdonald/mumu/target/Ding/ding_020910.pdf

[11] K.T. McDonald et al., *The MERIT High-Power Target Experiment at the CERN PS*, IPAC10 (May 26, 2010), http://www.hep.princeton.edu/~mcdonald/mumu/target/ipac10/wepe078.pdf

[12] T.W. Davies *et al., The production and anatomy of a tungsten powder jet*, Powder Tech. **201**, 296 (2010), http://puhep1.princeton.edu/~mcdonald/examples/accel/davies_pt_201_296_10.pdf

[13] R. Samulyak *et al., Computational algorithms for multiphase magnetohydrodynamics and applications to accelerator targets*, Cond. Matter Phys. **13**, no. 4, 43402 (2010), http://puhep1.princeton.edu/~mcdonald/papers/samulyak_cmp_13_4_43402_10.pdf

[14] A. Sou, S. Hosokawa and A. Tomiyama, *Effects of cavitation in a nozzle on liquid jet atomization*, Int. J. Heat Mass Trans.

50, 3575 (2007), http://puhep1.princeton.edu/~mcdonald/examples/fluids/sou_ijhms_50_3575_07.pdf
[15] N.V. Mokhov and A. Van Ginneken, *Pion Production and Targetry at μ+μ- Colliders*, (Dec 17, 1997), AIP Conf. Proc. 441, 320 (1998), http://www.hep.princeton.edu/~mcdonald/examples/accel/mokhov_aipcp_441_320_98.pdf
[16] J. Strait, N. Mokhov and S. Striganov, *Comparisons between MARS and HARP Data* (July 24 2009), http://www.hep.princeton.edu/~mcdonald/mumu/target/Strait/strait_marsvsharp.pdf
[17] The MIPP Experiment Upgrade (Fermilab P-960), http://ppd.fnal.gov/experiments/e907/Collaboration/P960/
[18] T. Davenne *et al*., *Mercury Beam Dump Simulations* (Dec. 15, 2008), http://www.hep.princeton.edu/~mcdonald/mumu/target/Davenne/davenne_121708.pdf
[19] See, for example, M. Rooney, *The Current T2K Beam Window Design* (Nov. 6, 2008), http://www.hep.princeton.edu/~mcdonald/mumu/target/Rooney/rooney_110608.pdf
[20] For a related concept, see C. Yoshikawa, C. Ankenbrandt, D. Neuffer, *Quasi-Isochronous Muon Collection Channels*, IPAC10, http://www.hep.princeton.edu/~mcdonald/mumu/target/ipac10/wepe073.pdf
[21] See, for example, S. Maloy *et al*., *Irradiation Effects in Tungsten and Tantalum*, http://puhep1.princeton.edu/~mcdonald/examples/accel/maloy_targetry_05.pdf
[22] C. Song, P. Wang and H.A. Makse, *A phase diagram for jammed matter*, Nature **453**, 629 (2008), http://puhep1.princeton.edu/~mcdonald/examples/detectors/song_nature_453_629_08.pdf
[23] A. Peles, http://www.rpi.edu/~pelesy/lib/research_interests.htm
[24] K.T. McDonald, Materials for the Target System Internal Shield (June 29, 2010), http://www.hep.princeton.edu/~mcdonald/mumu/target/targettrans74.pdf
[25] J.H. Schultz, Radiation Resistance of Fusion Magnet Materials, IEEE Symp. Fusion Eng. P. 423 (2003).
[26] R.B. Palmer, D.V. Neuffer and J. Gallardo, *A Practical High-Energy High-Luminosity $\mu^+\mu^-$ Collider*, AIP Conf. Proc. **335**, 635 (1995), http://puhep1.princeton.edu/~mcdonald/examples/accel/palmer_aipcp_335_635_95.pdf
[27] R.B. Palmer *et al*,. *Muon Colliders*, AIP Conf. Proc. **372**, 3 (1996), http://puhep1.princeton.edu/~mcdonald/examples/accel/palmer_aipcp_372_3_96.pdf
[28] M.A. Green, *Some Options for the Muon Collider Capture and Decay Solenoids,* AIP Conf. Proc. **372**, 100 (1996), http://puhep1.princeton.edu/~mcdonald/examples/accel/green_aipcp_372_100_95.pdf
[29] N.V. Mokhov, R.J. Noble and A. Van Ginneken, *Target and Collection Optimization for Muon Colliders*, AIP Conf. Proc. **372**, 61 (1996), http://puhep1.princeton.edu/~mcdonald/examples/accel/mokhov_aipcp_372_61_95.pdf
[30] K. Paul and C. Johnstone, *Optimizing the Pion Capture and Decay Channel*, MUC0289 (9 Feb. 2004), http://www.hep.princeton.edu/~mcdonald/mumu/target/Paul/paul_muc0289.pdf
[31] H. Takahashi *et al*., *Indirectly Cooled Radiation-Resistant Magnets for Hadron Target Station at J-PARC*, IEEE Trans. Appl. Supercon. **20**, 344 (2010), http://puhep1.princeton.edu/~mcdonald/examples/magnets/takahashi_ieeetas_20_344_10.pdf
[32] J.H. Schultz, *Radiation Resistance of Fusion Magnet Materials*, IEEE Symp. Fusion Eng. p. 423 (2003), http://puhep1.princeton.edu/~mcdonald/examples/magnets/schultz_ieeesfe_423_03.pdf